Jour. Petrol. Soc. Korea
Vol. 3, No. 1, p. 20~33, 1994

Subgrain boundaries in octachloropropane: deformation patterns, subgrain boundary orientation and density

Jin-Han Ree

Department of Geology, Kangwon National University, Chunchon 200-701, Korea

ABSTRACT : Some of the seven types of subgrain boundaries (Means and Ree, 1988) in octachloropropane samples show distinctive deformation patterns during their development. Type II subgrain boundaries migrate to accommodate the deformation difference between adjacent grains. The formation of Type III requires a rigid-body rotation of grains to reduce misorientation of adjacent grains. Types I, IV, V and VI develop either in static or dynamic condition. Type VII form only in static environments after deformation. Ribbon grains can develop via Type III or Type IV process. The orientation pattern and density of subgrain boundaries are more or less stable through a post-deformation heating. Subgrain boundary orientations are symmetric with respect to the grain-shape foliation in pure shear. In simple shear, their maximum inclines toward the direction of shear.

Key Words : Subgrain boundary, octachloropropane, deformation, ribbon grain

INTRODUCTION

Subgrains have been recognized as a typical microstructure of the deformation process at a relatively high temperature (Nicolas and Poirier, 1976; Poirier, 1985) and their size has been used extensively as a stress indicator (e.g. Twiss, 1977; White, 1977; Ord and Christie, 1984). Polygonization and kinking have been known to be two main processes responsible for the formation of subgrain boundaries (Nicolas and Poirier, 1976). However, Means and Ree (1988) found other processes also to form subgrain boundaries in experiments of an organic analog material, octachloropropane (hereafter called OCP). They described seven types of subgrain boundaries that are optically similar but which have different development histories. They also suggested that the presence of subgrains is not necessarily an indicator of deformation: i.e. they may form also in the static process without concomitant or previous deformation.

This paper is a further study of Means and Ree (1988), to present patterns of strain and particle motion associated with the formation of seven types of subgrain boundaries. The evolution of subgrain boundary orientation and length, and differences of subgrain boundary geometry between pure and simple shear are also discussed.

The subgrain boundaries described here are narrow (<10 μm wide) boundaries between parts of grains across which the extinction position differs abruptly by 1-8°. Subgrain boundaries of smaller misorientation than 1° may also have been present, but were not recognizable optically. In plane-polarized light, the image of a subgrain boundary vanishes. Grain boundaries, on the other hand, typically separate regions with bigger differences in extinction directions, and have distinct images even in plane light. In plane light, grain boundaries in OCP are marked by distinct dark lines or by brightness discontinuities (Means and Ree, 1988). These criteria of distinguishing subgrain boundaries from grain boundaries have also been used in the study of optical microstructures of natural rocks (e.g. Simpson and De Paor, 1991). Some boundaries in OCP samples are admittedly indeterminate as either grain boundaries or subgrain boundaries.

Table 1. Experimental conditions

Experiment	Deformation type	Strain rate (sec^{-1})	Total strain	Temperature (℃)	Duration of deformation(hr)
TO-11	Pure shear	2.0×10^{-5}	$-0.5(\varepsilon_3)$	70	6.94
TO-91	Simple shear	2.8×10^{-5}	$1.2(\gamma)$	70	12.17
TO-99	Pure shear	1.3×10^{-5}	$-0.3(\varepsilon_3)$	70	6.5
TO-100	Pure shear	2.3×10^{-5}	$-0.5(\varepsilon_3)$	100	6.17
TO-111	Simple shear	2.5×10^{-5}	$0.9(\gamma)$	80	9.5
TO-207	Simple shear	5.1×10^{-6}	$1.8(\gamma)$	80	99.63

*Axial strain rate for pure-shear experiments and shear strain rate for simple-shear experiments.

EXPERIMENTAL DESCRIPTIONS

Experiments were conducted using *synkinematic microscopy*-micoscopy during defomation (Means, 1989). It is an innovative approach to the study of microstructural developments in deforming materials. It was pioneered by Steinemann (1958), Rigsby (1960) and Wakahama (1964) in deforming ice and has been independently revived by several geologists recently (Means, 1977, 1980; Urai et al. 1980; Wilson, 1984). Various organic materials, ice and salt rocks have been used for synkinematic microscopy.

The material used in this study is OCP which is a soft, hexagonal organic material with a chemical formula of C_3Cl_8. It is optically uniaxial positive and has a melting point of 160℃. OCP generates optically very similar-looking microstructures to quartz (Means, 1983, 1989; Jessell, 1986; Means and Ree, 1988; Ree, 1990, 1991a, 1994; Jessell and Lister, 1991; Bons and Urai, 1992). The techniques of synkinematic microscopy and information about the experimental apparatus are given by Means (1989) in greater detail. Other techniques of sample preparation and measurements of deformation parameters, c-axis, grain size and grain-shape foliation are described by Ree (1991a).

In the subsections below, brief accounts of microstructural developments of each experiment will be described. The conditions of the experiments described in this paper are presented in Table 1.

Experiment TO-91

This simple shearing experiment was carried out at 70℃ or 0.8 Tm (Tm: absolute melting temperature) and at a shear strain-rate of about 2.8×10^{-5}/sec. A bulk shear strain of about 1.2 had been imposed for 12.17 hours, and then the sample had been heated statically at the deformation temperature for 15 hours on the deformation apparatus with the motor off but not backed-up. All seven types of subgrain boundaries were observed but only six types will be described in this sample since enough marker particles are not present for the other type. Evolutions of subgrain boundary orientation and length were also analyzed in this sample.

Fig. 1 shows three photomicrographs of the sample (a) at the beginning of the deformation, (b) immediately after the deformation, (c) after 15 hours of static heating. The main microstructural effects of the deformation were the introduction of an oblique grain-shape foliation at about 35° counterclockwise from the bulk shear direction with average grain axial ratio of 1.5, multiplication of subgrain boundaries more than twice and about 90% increase in average grain area from the initial average area of 1.0×10^{-2} mm^2. The average grain axial ratio at the end of the deformation ($\cong$1.5) is much lower than Rf value ($\cong$3.3) of bulk strain due to several foliation weakening processes described by Ree (1991a). The microstructural effects of static adjustment of 15 hours were limited further migration of grain boundaries eliminating some smaller grains which results in further increase

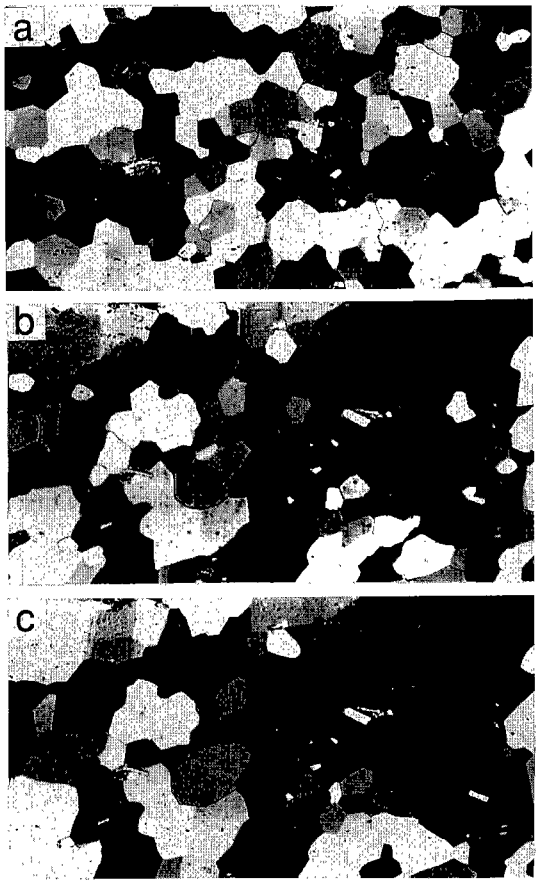

Fig. 1. Photomicrographs of sample TO-91 in cross-polarized light, (a) immediately before deformation, (b) 12.17 hr later, immediately after deformation when a bulk shear strain (γ) of about 1.2 has accumulated, and (c) after 15 hr of static adjustment at the deformation temperature. Fine black dots are marker particles (silicon carbide). The length of each photograph corresponds to 1.93 mm.

in average grain area by about 40%, some decrease in average grain axial ratio into 1.4, and local changes in subgrain geometry (Fig. 1c).

Other Experiments

The simple shearing experiment TO-207 was undertaken at a strain rate of 5.1×10^{-6}/sec and at 80℃ (0.8 Tm). This is the slowest experiment in this paper. A bulk shear strain of 1.8 had been imposed for 99.63 hours. After a bulk shear strain of about 0.5, strain became highly localized along a narrow band adjacent to the upper grip to develop ribbon grains (see Fig. 9). Only one type of subgrain boundaries (Type III of Means and Ree, 1988 and also see below) will be described although other types were also observed in the sample.

In pure shearing experiment TO-11 done by Means (1983), a bulk shortening (ε_3) of 50% was imposed at a strain rate of 2×10^{-5}/sec and at about 70℃. Microstructural developments in the sample were described by Means (1983, 1989). Type VI subgrain boundary (Means and Ree, 1988) will be described in this experiment because only this sample has enough marker particles for the deformation analyses associated with the development of Type VI subgrain boundary.

Orientations and lengths of subgrain boundaries were analyzed also in another simple shearing experiment (TO-111) and two pure shearing experiments (TO-99 and TO-100). In experiment TO-111, a bulk shear strain of 0.9 was accumulated at a shear strain-rate of 2.5×10^{-5} /sec and at 80℃. An oblique grain-shape foliation was developed at about 25° counterclockwise from the shear direction with an average grain axial ratio of 1.4.

Experiment TO-99 was done at a strain rate of 1.3×10^{-5}/sec and at 70℃. The total bulk strain (ε_3) was about 30%. A very weak grain-shape foliation developed at about 90° from the compression direction with an average grain axial ratio of 1.1.

Experiment TO-100 was undertaken at a higher temperature (100℃ ≅ 0.9 Tm) than other experiments. A bulk strain (ε_3) of 50% was imposed at a strain rate of 2.3×10^{-5}/sec and a grain-shape foliation with an average axial ratio of 1.3 was introduced at 90° from the compression direction.

RESULTS

The seven types of subgrain boundaries described by Means and Ree (1988) are shown schematically in Fig. 2. In this section, I will concentrate only on the deformation patterns

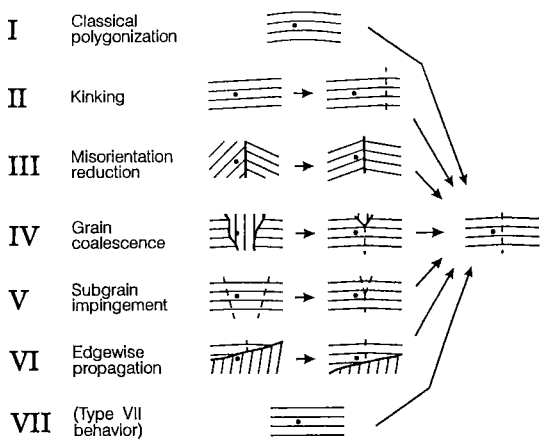

Fig. 2. Schematic representation of the seven types of subgrain boundary development. Heavy solid lines -grain boundaries. Dashed lines-subgrain boundaries. Light lines-traces of extinction direction at high angle to subgrain boundary (typically (0001) traces in OCP). Dot represents marker particle fixed in the material (after Means and Ree, 1988).

associated with the development of each type of subgrain boundaries. Analyses of subgrain boundary orientation and density, and the difference in the subgrain boundary geometry between pure shearing and simple shearing will also be shown in this section. More detailed descriptions of seven types of subgrain boundaries and their temporal development are given by Means and Ree (1988). The photomicrographs corresponding to some drawings of each type below are also shown by Means and Ree (1988).

Deformation Patterns

Type I subgrain boundaries

Type I boundaries develop by polygonization of bent crystals (Fig. 2). Type I boundary development does not require concurrent deformation of the grain, but this may occur as shown below.

Fig. 3 shows an example of Type I boundaries in the sample TO-91 with marker particle trajectories and strain ellipses. At the stage of Fig. 3a, a bulk shear strain of 0.8 has been accumulated in the sample. With a progressive deformation, the grain shows an undulose extinction (not shown in Fig. 3b) and then there develop six subgrain boundaries of Type I in the NE and SW corners of the grain (Fig. 3d). A continuous change in the interference color through subgrains from SW to NE within the grain indicates that these subgrain boundaries develop by polygonization. The grain at the end of the deformation interval shown in Fig. 3 looks like a 'porphyroclast with tails' although the grain here shows a slightly net growth in the total area. Intragranular strain ellipses reveal a strain gradient from the SW to NE corner of the grain (Figs. 3c and e). Subgrain boundaries develop both in the lowest and highest strained areas. In the low strained area (SW corner), the grain boundary at a high angle to the grain long axis migrates away from the grain to develop a 'tail'. In the high strained area (NE corner), on the other hand, grain boundaries at a low angle to the grain long axis migrate toward the grain to form a 'tail'.

Type II subgrain boundaries

Type II boundaries are essentially kink band boundaries, which migrate through a grain during deformation (Fig. 2). Fig. 6 shows marker particle trajectories and strain ellipses within a grain forming a Type II boundary in the sample TO-91. With progressive deformation the subgrain boundary migrates to the left with some syn-migration straining on either side of the subgrain boundary. The direction of the long axis of the strain ellipse is noticeably different for the two sides and the boundary probably migrates sidewise to accommodate deformation difference across it, as explained by Means and Jessell (1986).

Type III subgrain boundaries

Type III boundaries form more or less *in situ* (without migration) at the sites of former grain boundaries, by reduction of lattice misorientation between neighboring grains (Fig. 2). This process was named *amalgamation* by Means (1989). Type III behavior is one way of increasing grain size

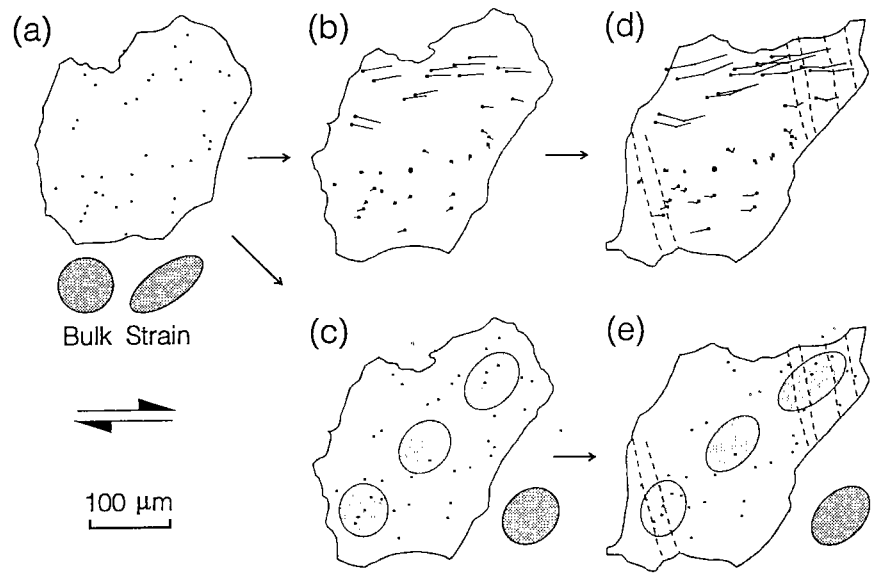

Fig. 3. Maps showing development of Type I subgrain boundaries (dashed lines) in sample TO-91. (b) and (d) show marker particle trajectories with a fixed marker particle within the grain (solid circle). Small circles represent initial positions of marker particles. (c) and (e) show intragranular strain ellipses and bulk strain ellipses around the grain of additional deformations accumulated from (a). Bulk strain ellipse in (a) represents strain of the sample from the beginning of the deformation. Reference circle for ellipses is also shown in (a).

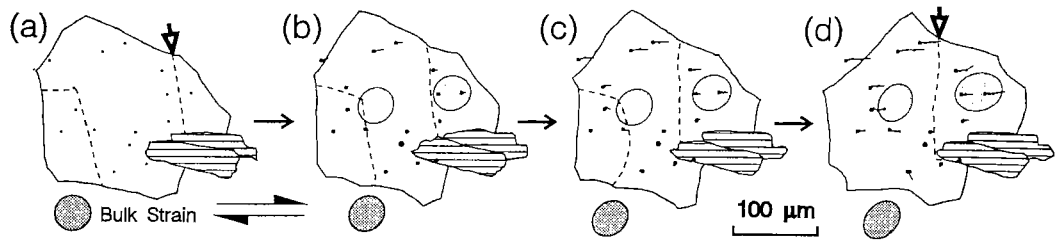

Fig. 4. Maps of marker particle trajectories and intragranular and bulk strains around a grain developing Type II subgrain boundary in sample TO-91. Type II subgrain boundary is marked with a pointer in (a) and (d). Solid circle is a fixed point for trajectories. Stage (a) is at the beginning of the deformation. Ornamented fragments are bits of papers incorporated accidentally.

during dynamic recrystallization. It is believed that Type III behavior requires concurrent deformation.

In an example of the sample TO-91 (Fig. 5), marker particle trajectories within the upper grain (grain 30) with a fixed point in grain 42 show a rotating pattern in the earlier stage of the sequence (Fig. 5b). A rotation of lattice plane of grain 30 is also indicated by the change in orientation of two subgrain boundaries within the grain (Fig. 5c).

When Type III behavior occurs along a grain boundary at a high angle to the grain long axis in simple shearing experiments, it usually develops a ribbon grain. Fig. 6 shows a progressive development of ribbon grains in the sample TO-207. At the stage of Fig. 6a, the sample has already undergone a bulk shear strain of 1.4. The deflection of marker lines drawn almost perpendicular to the bulk shear direction at the beginning of the sequence, and intragranular strain ellipses indicate a strong localization of

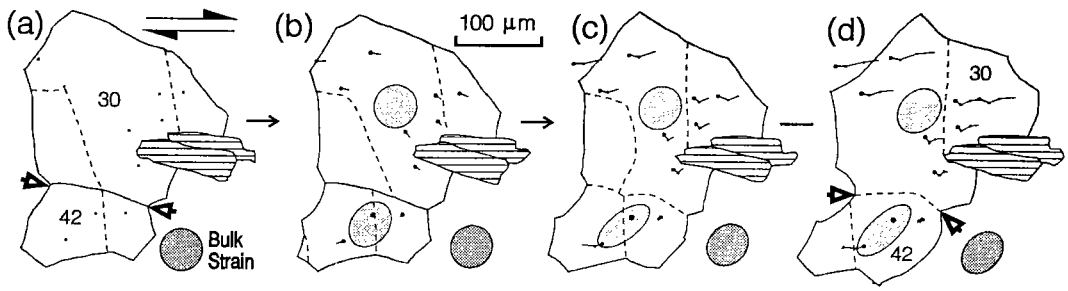

Fig. 5. Maps showing development of Type III subgrain boundary (with paired pointers in (d)) between grains 30 and 42 (numbered), marker particle trajectories, intragranular strain, and bulk strain around the grain in sample TO-91. Solid circle is a fixed point for trajectories. Stage (a) is at the beginning of the deformation. Ornamented fragments are bits of papers incorporated accidentally.

deformation along a band adjacent to the upper grip (Fig. 6d). In the lower half of the sample, grains show almost no straining although some local changes in the configuration of grain and subgrain boundaries occur. In the high strain zone, amalgamations between grains 1 and 2, and between grains 4 and 5 form ribbon grains with their long axes oblique both to the bulk shear direction and grain-shape foliation. The lower boundaries of these ribbon grains do not show any noticeable migration into the low strain zone although the lower boundary of grain 5 shows some back-and-forth migration into the low strain zone. The measurement of the trend of c-axes of these grains on a flat stage during deformation confirmed a near parallelism of the trend of their basal slip planes to the bulk shear direction.

Type IV subgrain boundaries

Type IV boundaries develop by coalescence of two grains with similar lattice orientations which were not initially in contact with each other, but which become neighbors by consuming intervening grains with grain boundary migration (Fig. 2). Thus, Type IV behavior can occur whenever grain boundary migration can occur (i.e. in static or dynamic environments). Type IV behavior is another way of increasing grain size during dynamic recrystallization. Ribbon grains can also form by this process as shown in a deforming paradichlorobenzene sample by Urai *et al.* (1986, fig. 29).

In a dynamic example of Type IV in the sample TO-91 (Fig. 7), boundaries of two grains (8 and 10) migrate toward each other by consuming the intervening portion of grain 9, to form a Type IV boundary. A static example has been illustrated by Means and Ree (1988).

Type V subgrain boundaries

Type V boundaries form by impingement of migrating subgrain boundaries (Fig. 2). They are similar in principle to Type IV, but in Type V subgrain boundaries migrate instead of grain boundaries.

Fig. 8 shows a dynamic example of the sample TO-91 where one subgrain boundary (the right one of the two subgrain boundaries) migrates and impinges on the other one to form a T junction while the grain is deforming. A static example has been shown by Means and Ree (1988).

Type VI subgrain boundaries

Type VI boundaries are portions of boundaries that have propagated in their own planes behind migrating grain boundaries to which they are attached (Fig. 2). They are believed to develop as a simple consequence of the outward growth of the two adjoining subgrains. Therefore, they can occur in static or dynamic environments. Static examples were described in OCP samples by Means and Dong (1982), who referred to the process as "edgewise propagation" of subgrain boundaries.

Fig. 9 shows a dynamic example of Type VI in

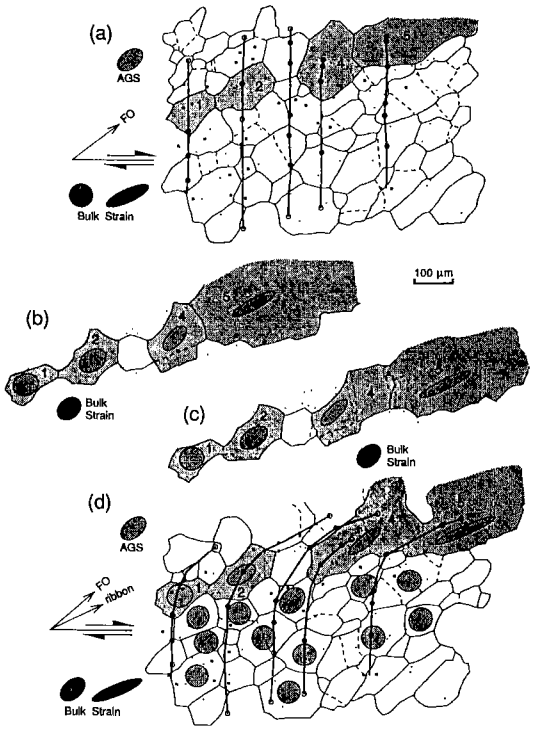

Fig. 6. Maps showing development of Type III subgrain boundaries between grains 1 and 2, and between grains 4 and 5 in sample TO-207. In (a), a bulk shear strain of about 1.4 has been already imposed from the beginning of the deformation. Intragranular and bulk strain ellipses in (b), (c) and (d) represent additional strains accumulated form (a). In (d) total bulk strain ellipse (marked as T) is also shown. Material lines (thick lines) were drawn almost perpendicular to the bulk shear direction at the beginning of the sequence by connecting real marker particles (circles) and imaginary marker positions (not shown) calculated by interpolating positions of adjacent marker particles (smaller circles). Average grain shape (AGS) and orientation of grain-shape foliation (FO) calculated with projection method (Panozzo, 1983) are also shown in (a) and (d).

the sample TO-11 deformed by pure shear. At the stage of Fig. 9a, the sample has been shortened in the E-W direction by 35%. With an additional shortening of about 15%, the outer extremities of the subgrain boundary propagate in the shortening direction with Type VI behavior, which cannot be explained by plastic extension of the grain in the shortening direction. Type VI behavior may involve some migration of the subgrain boundary as well as its edgewise extension. This is the case in Fig. 9 where the subgrain boundary migrates to the south as well as propagates in the E-W direction. The example of Means and Dong (1982) also shows a migration of the subgrain boundary.

Type VII subgrain boundaries

Type VII boundaries develop statically from optically "strain-free" grains (grains with uniform interference color and intensity and uniform extinction), by a process probably otherwise similar to the Type I process (Fig. 2 and also see fig. 4g-i of Means and Ree, 1988). Indeed, there were no marker particle movements with the development of Type VII and thus no deformation in the observation scale of this study.

Subgrain Boundary Orientation and Density

Subgrain boundary orientation of each type

Orientations of subgrain boundaries of each type were measured from digitized images in sample TO-91. To draw rose diagrams, lengths of subgrain boundaries were summed at 5° intervals and the total length of each orientation was divided by the maximum length to normalize it. Since some subgrain boundaries have changed their orientation throughout the deformation, orientations of subgrain boundaries were measured from photographs at one hour intervals for the deformation period. For the static period, only the last stage (at 15 hours after the deformation) was measured.

Fig. 10 shows rose diagrams of each type. Types I and II show a strong preferred orientation perpendicular to the bulk shear direction. Type III subgrain boundaries show a broad orientation but with a low concentration at 120-170° from the bulk shear direction. Type IV boundaries tend to lean toward the bulk shear direction. Types V, VI, and VII show a preferred orientation at a high angle to the shear direction. However, preferred orientations of Types IV, V, VI, and VII are of uncertain significance since their populations are relatively minor.

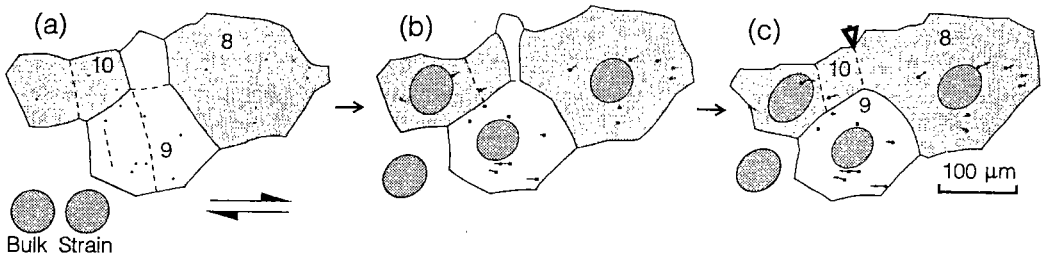

Fig. 7. Maps showing development of Type IV subgrain boundary (with a pointer in (c)) in sample TO-91. At stage (a) a bulk shear strain of less than 0.1 has been imposed from the beginning of the deformation, and strain ellipse (right) and reference circle (left) look almost the same. Bulk strain ellipse in (b) and (c) represents additional strain of the area around the grains shown. Intragranular strain ellipses also represent additional strains from (a). In (b) and (c) a small solid circle in grain 9 represents a fixed marker particle for marker particle trajectories.

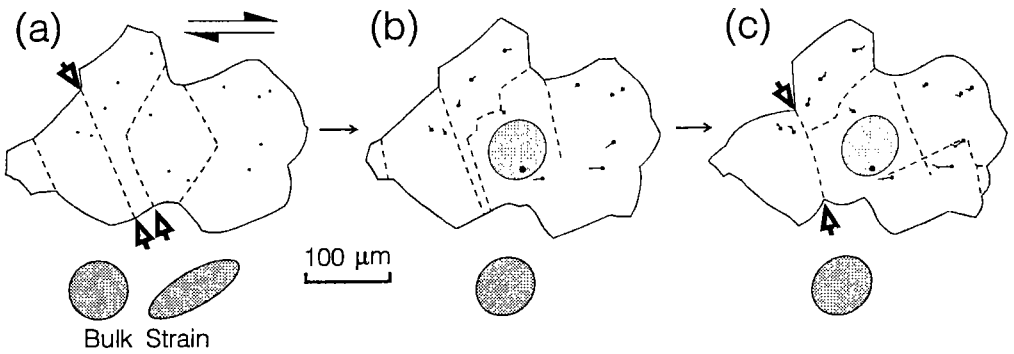

Fig. 8. Maps showing development of Type V subgrain boundary by impingement of two subgrain boundaries (with pointers in (a) and (c)) in sample TO-91. Bulk strain ellipses represent strain of the sample from the beginning of the deformation in (a), and additional strains around the grain from (a) in (b) and (c). Intragranular strain ellipses also represent additional strains from (a). Solid circle represents a fixed marker particle for marker particle trajectories in (b) and (c).

Evolution of subgrain boundary orientation

Rose diagrams of Fig. 11 show the evolution of subgrain boundary orientations in the sample TO-91. For these diagrams, orientations of all subgrain boundaries, whether they display a certain type or not, were measured. At the beginning of the deformation the sample already had subgrain boundaries developed during sample preparation. They show a strong preferred orientation at a high angle to the bulk shear direction, which probably reflects a preferred flow of OCP along the shear zone window during sample pressing. Throughout the deformation, subgrain boundaries maintain a more or less constant preferred orientation with the maximum at about 90° and the minor one at a low angle to the shear direction. At the end of the deformation (Fig. 11g), the minor preferred orientation is about parallel to the grain-shape foliation. After 15 hours of static heating, the preferred orientation does not show much change although the minor preferred orientation tends to be broader.

Evolution of subgrain boundary density

The length of subgrain boundaries were measured also from digitized images in the sample TO-91. The total length of each measured stage was divided by the mapped area, the value of which is referred to here as *subgrain boundary*

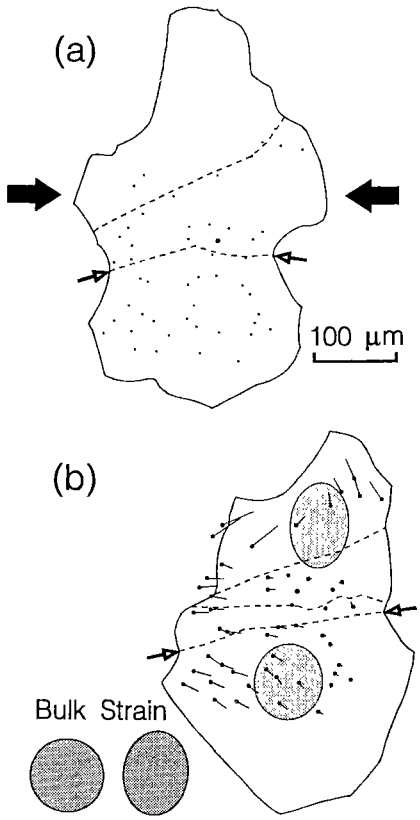

Fig. 9. Maps showing edgewise propagation of subgrain boundary (with pointers; Type VI) in sample TO-11 from experiment by Means (1983). In (a) a bulk shortening of the sample is about 35%. Bulk strain ellipse in (b) represents additional strain around the grain shown from (a). Intragranular strain ellipses and marker particle trajectories are also shown in (b). Bulk shortening direction is horizontal.

density. Fig. 12 shows a plot of subgrain boundary density against bulk shear strain. The initial density of about 2.2 mm^{-1} tends to increase with the deformation and reaches to about 5.1 mm^{-1} (more than doubling from the beginning) at the end of the deformation, although it shows some decrease after a bulk shear strain of about 1.1. With a static heating of 15 hours, the sample shows some increase in subgrain boundary density (less than 0.4 mm^{-1}).

Comparison of subgrain boundaries between pure shear and simple shear

Subgrain boundary orientations of two simple-sheared and two pure-sheared samples were measured at the end of each deformation, and are shown as rose diagrams in Fig. 13 with the foliation orientation as a reference horizontal axis.

In simple-sheared samples, the preferred orientation of subgrain boundaries is oblique to the grain-shape foliation but about perpendicular to the shear direction. A weak, minor preffered oriontation tends to be parallel to the grain-shape foliation and oblique to the maximum preferred orientation.

In pure-sheared samples, on the other hand, the preferred orientation of subgrain boundaries is about perpendicular to the grain-shape foliation and its range is somewhat broader than in simple-sheared samples. The minor preferred orientation tends to be parallel to the grain-shape foliation as in simple-sheared samples but with a somewhat broader range and at a higher angle to the maximum preferred orientation.

Fig. 14 shows a plot of the subgrain boundary density against the axial ratio of bulk strain ellipse (Rf) for the samples mentioned above. Subgrain boundary densities of one pure-sheared sample (TO-100) and two simple-sheared samples are in the range of 5-6 mm^{-1}, but the other pure-sheared one (TO-99) shows much higher density than others even with a lower Rf.

DISCUSSION

Means and Ree (1988) classified subgrain boundaries into seven types by their structural history. In sample TO-91, three fourths of the boundaries are Type I (classical polygonization), Type II (kinking) and Type III (misorientation reduction) (Means and Ree, 1988). Types I, II, III, IV, and VII are essentially *generating types* which create subgrain boundaries. Type V, on the other hand, is a *diminishing type* in which the total length of subgrain boundaries (or density) decreases by impingement of two subgrain boundaries. Type VI behavior (edgewise propagation) has the effect of increasing the

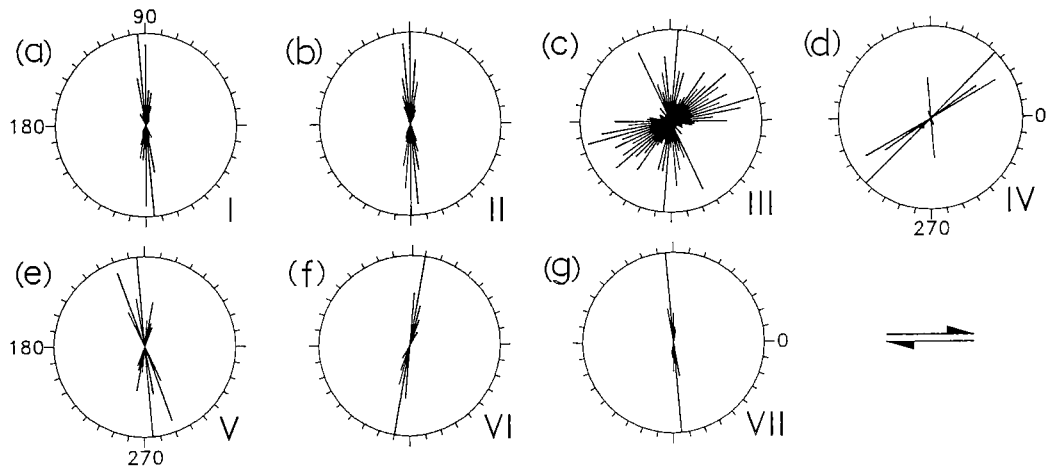

Fig. 10. Rose diagrams showing orientations of subgrain boundaries of each type in sample TO-91. Total length of subgrain boundaries measured on the true scale is (a) 9.43 mm, (b) 10.06 mm, (c) 9.22 mm, (d) 0.33 mm, (e) 0.25 mm, (f) 0.28 mm, and (g) 5.71 mm. Bulk shear direction horizontal.

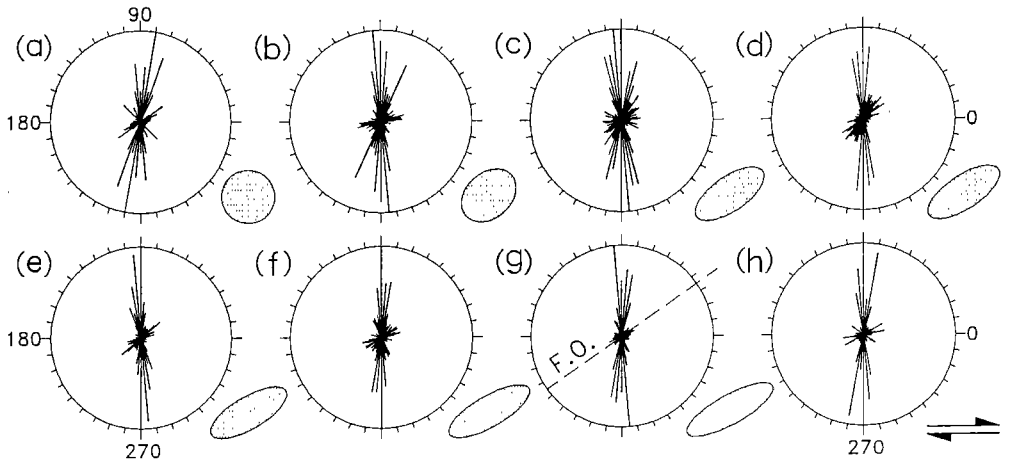

Fig. 11. Rose diagrams showing evolution of subgrain boundary orientations in sample TO-91. (a) Before deformation. Bulk shear strains (γ) are (b) 0.3, (c) 0.8, (d) 0.9, (e) 1.0, (f) 1.1, and (g) 1.2 (after deformation), (h) After 15 hours of the static interval. Bulk strain ellipses are also shown at each stage. F.O. in (g) indicates foliation orientation.

length of pre-existing subgrain boundaries (*multiplication type*).

The development of Types II and III requires concurrent deformation. Type II boundaries migrate sidewise to accommodate deformation incompatibility between adjacent subgrains (Fig. 4 and see also Means and Jessell, 1986). Marker particle trajectories and deformation pattern confirm that some component of rigid-body rotation of grains in the deformation is necessary for the formation of Type III (Fig. 5). Type VII, on the other hand, form only in static environments after deformation. Types I, IV, V and VI can develop in static or dynamic environments.

Orientation analyses of subgrain boundaries of each type in the sample TO-91 show that Types I, II, V, VI, and VII have an orientation similar

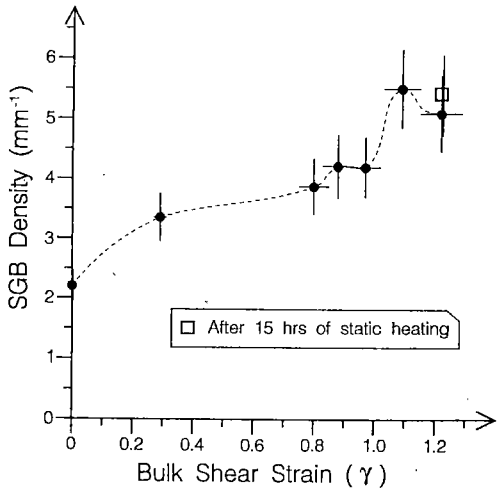

Fig. 12. Plot of subgrain boundary density against bulk shear strain in sample TO-91. Vertical and horizontal bars represent ranges of measurement errors of subgrain boundary density and ±1 standard deviation of bulk shear strains, respectively.

to each other, but Types III and IV have different orientation patterns. Discussions of only Types I, II and III orientations are meaningful because the population of the other types is relatively minor. The preferred orientation of Types I and II, perpendicular to the bulk shear direction, is believed to be strongly related to easy slip planes parallel to the shear direction. Although c-axis orientations were not measured in the sample TO-91, c-axis measurements in other simple shearing experiments confirmed that Types I and II boundaries are mostly prismatic subgrain boundaries (Ree, 1991b). The broad pattern of Type III orientation suggests that grain boundaries in any orientation can turn into subgrain boundaries as long as the difference in lattice orientation between neighboring grains are reduced. However, the reason why Type III boundaries show some vacancy in orientation at 120-170° from the shear direction is not clear. One possible explanation is that grain boundaries in this orientation became relatively minor in frequency as the sample was deformed (this was confirmed by analyses of grain boundary orientation), and that grain boundaries with this orientation may have rotated before they turned into subgrain boundaries.

The analysis of subgrain boundary density in the sample TO-91 shows that the density increased by about 130% during the bulk shear strain of 1.2. At 15 hours after the (12-hour) deformation was finished, with the sample still at the deformation temperature, the subgrain boundary density shows only a 6% increase and the orientation of subgrain boundaries remains more or less unchanged. These observations indicate that the density and orientation of subgrain boundaries are quantities which could be called a post-tectonic annealing. The post-deformational development of Type VII subgrain boundaries in sample TO-91 seems

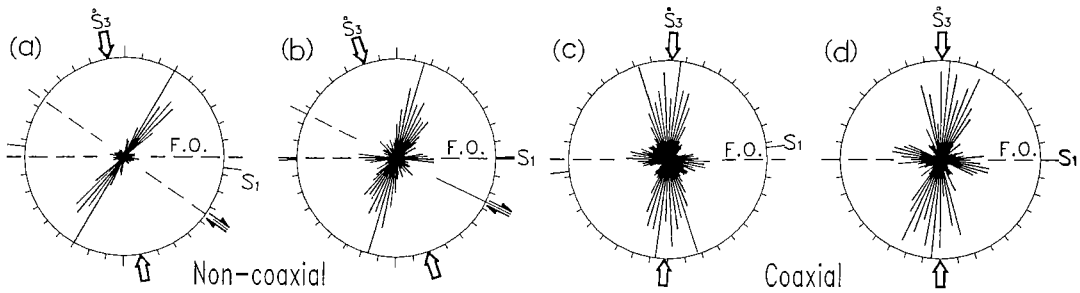

Fig. 13. Rose diagrams of subgrain boundary orientations of samples (a) TO-91, (b) TO-111, (c) TO-99, and (d) TO-100 at the end of deformation, with the foliation orientation (F.O.) as a reference horizontal axis. S1: maximum finite stretch direction. $\dot{S}_3$: shortening direction, assuming $\dot{S}_3$ to be at about 45° to the bulk shearing direction in simple shearing experiment ((a) and (b)) and to be parallel to the bulk compression direction in pure shearing experiment ((c) and (d)).

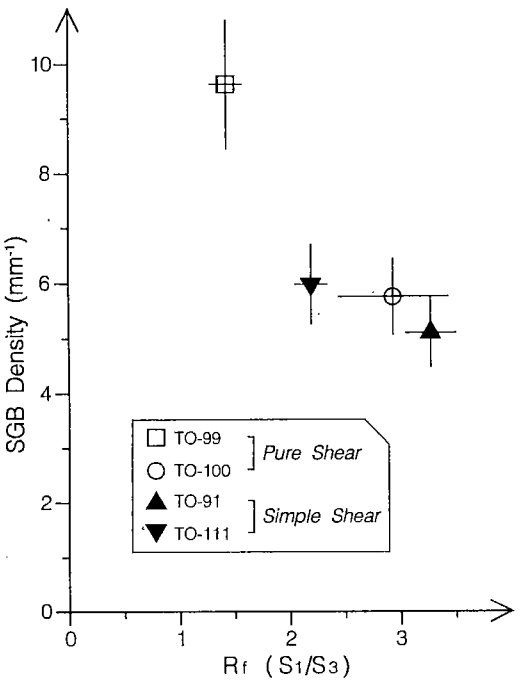

Fig. 14. Plot of subgrain boundary density against bulk Rf in two pure-sheared and two simple-sheared samples. Vertical and horizontal bars represent ranges of measurement errors of subgrain boundary density and ±1 standard deviation of bulk Rf, respectively.

however to contradict to this. Almost all Type VII subgrain boundaries in this sample, however, formed parallel to an existing preferred orientation of subgrain boundaries and some pre-existing subgrain boundaries disappeared during the static heating. These two effects allowed the orientation and density of the subgrain boundaries in the sample to remain more or less stable during the post-deformation period.

Quartz ribbons in naturally deformed rocks have been interpreted as a result of either elongation of original grains (Wilson, 1975; Bouchez, 1977; McLelland, 1984; Law *et al.*, 1986) or oriented dynamic grain growth (Bouchez *et al.*, 1984; Culshaw and Fyson, 1984). Ribbon grains can also develop by grain coalescence (Type IV) as shown by Urai *et al.* (1986), or by amalgamation (Type III) as seen earlier in this paper.

In pure-sheared samples, subgrain boundary orientations tend to be symmetric with respect to the grain-shape foliation. In simple-sheared samples, on the other hand, they are asymmetric with respect to the grain-shape foliation. This may suggest that subgrain boundary orientation could be a possible criterion distinguishing pure shear from simple shear deformation. Also the leaning of the maximum orientation towards the grain-shape foliation in simple-sheared samples may be a possible sense-of-shear indicator. The obliquity of the maximum orientation to the grain-shape foliation is because most of boundaries are prismatic subgrain boundaries resulting from dominant basal slip and because basal slip planes tend to align parallel to the bulk shear plane.

Subgrain boundary densities of three samples (one pure- and two simple-sheared ones) are in the range of 5-6 mm^{-1} with the other pure-sheared sample (TO-99) showing a much higher value. It is not clear why the sample TO-99 has a higher density at present. More data are needed to discuss any similarity or difference in subgrain boundary density between pure- and simple-sheared samples.

There are some limitations of the study of subgrain boundaries under optical microscopy. First, it is difficult to recognize subgrain boundaries of smaller misorientations than 1° under optical microscopy as explained earlier. Another limitation is that prismatic subgrain boundaries resulting from prism ⟨**a**⟩ slip cannot be seen under optical microscopy since subgrains either side of the boundary will have the same c-axis orientation (Trepied *et al.*, 1980). However, the pattern of c-axis fabrics and marker particle trajectories suggest that prism ⟨**a**⟩ slip is only minor in deforming OCP samples (Ree, 1991b).

For a better understanding of each type of subgrain boundaries in OCP samples, the lattice orientation should be related with developments of subgrain boundaries. Unfortunately, c-axes were not measured in the experiment TO-91. The measurement of c-axes before, during and after deformation will help to study the development of subgrain boundaries more precisely in the

future.

CONCLUSIONS

(1) The development of Types II and III subgrain boundaries in octachloropropane samples requires concurrent deformation. Type VII forms only during static heating after deformation. Types I, IV, V and VI can develop statically or dynamically.

(2) Types I and II are mostly prismatic subgrain boundaries resulting from basal slip.

(3) Ribbon grains can develop by misorientation reduction (Type III) or by grain coalescence (Type IV).

(4) The orientation and density of subgrain boundaries are more or less stable through a static heating after deformation.

(5) Subgrain boundary orientations are symmetric with respect to the grain-shape foliation in pure shear, whereas they are asymmetric with respect to the grain-shape foliation in simple shear.

(6) The obliquity of the maximum of subgrain boundary orientations to the grain-shape foliation (i.e. leaning in the direction of shear) can be a possible sense-of-shear indicator, where one slip system is dominant.

ACKNOWLEDGMENTS

This work is part of a Ph.D. thesis at the University of New York at Albany. Valuable suggestions by W. D. Means during the study are greatly appreciated. I thank T. W. Chang, S.-G. Hwang, S.-T. Kwon, and an anonymous reviewer for their constructive comments on the manuscript. This work was supported by NSF grant EAR 9003954 to W. D. Means. Partial funding for the publication was provided by the Center for Mineral Resources Research (CMR).

REFERENCES

Bons, P. D. and Urai, J. L., 1992, Syndeformational grain growth: microstructures and kinetics. J. Struct. Geol., 14, 1101-1109.

Bouchez, J. L., 1977, Plastic deformation of quartzites at low temperature in an area of natural strain gradient. Tectonophysics, 39, 25-50.

Bouchez, J. L., Mainprice, D. H., Trepied, L. and Doukhan, J. C., 1984, Secondary lineation in a high-T quartzite (Galicia, Spain): an explanation for an abnormal fabric. J. Struct. Geol., 6, 159-165.

Culshaw, N. G. and Fyson, W. K., 1984, Quartz ribbons in high grade granite gneiss: modifications of dynamically formed quartz c-axis preferred orientation by oriented grain growth. J. Struct. Geol., 6, 663-668.

Jessell, M. W., 1986, Grain boundary migration and fabric development in experimentally deformed octachloropropane. J. Struct. Geol., 8, 527-542.

Jessell, M. W. and Lister, G. S., 1991, Strain localization behavior in experimental shear zones. Pure Appl. Geophys., 137, 421-438.

Law, R. D., Casey, M. and Knipe, R. J., 1986, Kinematic and tectonic significance of microstructures and crystallographic fabrics within quartz mylonites from the Assynt and Eriboll regions of the Moine thrust zone, NW Scotland. Trans. R. Soc. Edinb., Earth Sci., 77, 99-125.

McLelland, J. M., 1984, The origin of ribbon lineation within the southern Adirondacks, U. S. A. J. Struct. Geol., 6, 147-157.

Means, W. D., 1977, A deformation experiment in transmitted light. Earth Planet. Sci. Lett., 35,169-179

Means, W. D., 1980, High temperature simple shearing fabrics; a new experimental approach. J. Struct. Geol., 2, 197-202.

Means, W. D., 1983, Microstructure and micromotion in recrystallization flow of octachloropropane: a first look. Geol. Rdsch., 72, 511-528.

Means, W. D., 1989, Synkinematic microscopy of transparent polycrystals. J. Struct. Geol., 11, 163-174.

Means, W. D. and Dong, H. G., 1982, Some unexpected effects of recrystallization of the microstructure of materials deformed at high temperature. Mitt. Geol. Inst. der E. T. H., Neue Floge, 239a, 205-207.

Means, W. D. and Jessell, M. W., 1986, Accommodation migration of grain boundaries. Tectonophysics, 127, 67-86.

Means, W. D. and Ree, J.-H., 1988, Seven types of subgrain boundaries in octachloropropane. J. Struct. Geol., 10, 765-770.

Nicolas, A. and Poirier, J. P., 1976, Crystalline Plasticity and Solid State Flow in Metamorphic Rocks. Wiley, New York, 444p.

Ord, A. and Christie, J. M., 1984, Flow stresses from microstructures in mylonitic quartzites from Moine Thrust Zone, Assynt area, Scotland, J. Struct. Geol., 6, 639-654.

Panozzo, R., 1983, Two-dimensional analysis of shape fabric using projections of lines in a plane.

Tectonophysics, 95, 279-294.
Poirier, J. P., 1985, Creep of Crystals. Cambridge University Press, Cambridge, 260p.
Ree, J.-H., 1990, High temperature deformation of octachloropropane: dynamic grain growth and lattice reorientation. In: Deformation Mechanisms, Rheology and Tectonics (edited by Knipe, R. J. and Rutter, E. H.). Spec. Publs geol. Soc. Lond., 54, 363-368.
Ree, J.-H., 1991a, An experimental steady-state foliation. J. Struct. Geol., 13, 1001-1011.
Ree, J.-H., 1991b, High temperature deformation of octachloropropane: a microstructural study. Unpublished Ph.D. thesis, State University of New York at Albany, 227p.
Ree, J.-H., 1994, Grain boundary sliding and development of grain boundary openings in experimentally deformed octachloropropane. J. Struct. Geol., 16, 403-418.
Rigsby, G. P., 1960, Crystal orientation in glaciers and experimentally deformed ice. J. Glaciol., 3, 589-606.
Simpson, C. and De Paor, D., 1991, Deformation and Kinematics of High Strain Zones. Short Course Notes, 1991 Annual GSA Meeting, 116p.
Steinemann, S. Von., 1958, Experimentelle untersuchung zur plastizitat von eis. Beit zur Geol. der Schweiz, Hydrologie, 10, 4-10.
Trepied, L., Doukhan, J. C. and Paquet, J., 1980, Subgrain boundaries in quartz: theoretical analysis and microscopic observations. Phys. Chem. Min., 5, 201-218.
Twiss, R. J., 1977, Theory and applicability of a recrystallized grain size paleopiezometer. Pure Appl. Geophys., 115, 227-244.
Urai, J. L., Humphreys, F. J. and Burrows, S. E., 1980, In situ studies of the deformation and dynamic recrystallization of rhombohedral camphor, J. Mater. Sci., 15, 1231-1240.
Urai, J. L., Means, W. D. and Lister, G. S., 1986, Dynamic recrystallization of minerals. In: Mineral and Rock Deformation: Laboratory Studies-The Paterson Volume (edited by Heard, H. C. and Hobbs, B. E.). Am. Geophys. Un. Geophys. Monogr., 36, 161-199.
Wakahama, G., 1964, On the plastic deformation of ice V, Plastic deformation of polycrystalline ice. Low Temperature Sci., 22, 1-24.
White, S., 1977, Geological significance of recovery and recrystallization processes in quartz. Tectonophysics, 39, 143-170.
Wilson, C. J. L., 1975, Preferred orientation of quartz ribbon Mylonites. Bull. Geol. Soc. Am., 86, 968-974.
Wilson, C. J. L., 1984, Shear bands crenulations, and differentiated layering in ice-mica models. J. Struct. Geol., 6, 303-319.

(책임편집 : 황상기)

옥타클로로프로페인의 아입자경계 : 변형 형태, 아입자경계 방향과 밀도

이 진 한

강원대학교 지질학과

요 약: Means and Ree (1988)에 의해 보고된 옥타클로로프로페인 (octachloropropane) 시료의 일곱 종류 아입자경계중 일부는 형성시 특징적인 변형 형태를 보여준다. II형의 아입자경계는 인접 아입자간의 변형차를 조절하기 위하여 이동한다. III형의 형성에는 인접 입자간의 격자 오방향차를 줄이기 위한 입자의 강성체 회전이 필수적이다. I, IV, V, VI형의 아입자경계는 변형의 유무에 관계없이 발달할 수 있다. 반면에 VII형은 변형 후 정적인 상태에서만이 형성 가능하다. 리본입자는 III이나 IV형의 과정을 통해서도 발달할 수 있다. 아입자경계의 방향과 밀도는 변형 후 열 작용시에 다소 안정한 특성을 보여준다. 아입자경계 방향은 순수전단시 입자형태엽리에 대해 대칭적이나 단순전단시에는 비대칭적이며 그 최대치는 전단 방향 쪽으로 기울어짐을 보인다.

핵심어 : 아입자경계, 옥타클로로프로페인 (octachloropropane), 변형, 리본입자